Short communication

On the stress tensor in Vrancea region

M.C. Oncescu

Centre of Earth Physics and Seismology, P.O. Box MG-2, Bucharest-Magurele, Romania

Introduction

Vrancea region (Romania) is a complex tectonic zone characterized by a clustered but intense intermediate-depth seismic activity and by a 'continent-continent-like' collision between three tectonic units (East-European Platform, Moesian Sub-plate and Inter-Alpine Sub-plate) which leads also to moderate-size crustal earthquakes. Both crustal and sub-crustal events present some diversity in focal mechanisms that made early seismotectonic interpretation difficult (Roman, 1970; Ritsema, 1974).

As was shown by McKenzie (1969), if there are pre-existing zones of weakness on which slip can occur, the directions of the principal stresses σ_1, σ_2, σ_3 may not be close to the P, B and T axes from focal mechanisms. In such cases, only the direction and sense of resolved shear stress on the fault plane, as indicated by the slip vector, can be used to constrain the stresses. Assuming that the variety of focal mechanisms are consistent with a single regional stress tensor, Gephart and Forsyth (1984) developed a new inverse technique to seek a uniform stress field that predicts directions and senses of slip in agreement with the observations.

The aim of this short note is (1) to present a new application of this attractive method, (2) to point out that in Vrancea region the compression axis acts in a NE–SW direction and not in a SE–NW direction, as is commonly thought from focal mechanism results, and (3) to give additional evidence that the stresses in the crust are decoupled from those in the subducted slab.

Method and data

Gephart and Forsyth (1984) chose to describe the deviatoric part of the model stress tensor by four independent parameters, the directions of the principal stress axes $\sigma_1 < \sigma_2 < \sigma_3$ and the ratio $R = (\sigma_2 - \sigma_1)/(\sigma_3 - \sigma_1)$, thus dealing only with shear-stress directions on the fault planes and neglecting shear-stress magnitudes and hydrostatic stress. This parameterization is particularly useful for data sets for which P and T axes from focal mechanism (principal strain axes) are not well clustered. The ratio R specifies the magnitude of σ_2 relative to σ_1 and σ_3, and is defined between 0 and 1, both situations describing a bi-axial stress state.

The inversion is performed by a grid search over the three stress directions (characterized by three independent angles) and R, looking for the minimization of the sum of absolute values of the rotation angles about any axis needed to bring the observed and predicted slip direction and senses into coincidence. When the fault plane is not known 'a priori', there are two rotation angles for the two nodal planes. Thus, in performing the inversion, one selects the plane that is more consistent with the stress model. The inversion is performed in two steps: first, the whole stress model space is searched, on a 10°–15° grid for angles and 0.1 units for R, using an approximate method (the rotation axes were pre-specified to be the poles of the two nodal planes and the null vector); second, the exact method (with the much more time-consuming determination of the minimum rotation axes) was applied in the vicinity of the isolated minima.

The data set consists of two sub-sets: one is formed by 27 intermediate-depth earthquakes (see Table 1) which occurred between 1934 and 1986 with magnitudes in the range $5.0 \leq M \leq 7.4$ (with one exception, and M 4.0 event on May 16, 1982 at about 200 km depth); the other sub-set is formed by 12 crustal events (see Table 2) which occurred between 1959 and 1986 with $4.0 \leq M \leq 5.4$ (with one exception, an M3.0 event on April 27, 1986 in Vrancea foredeep). The first sub-set consists of fault-plane solutions obtained with a minimum of 20 and an average of 65 P-wave first motion signs (Fig. 1); the solutions of the second sub-set were obtained with a minimum of 15 and an average of 39 signs (Fig. 2). The fault-plane solutions were determined with short-period P-wave first motion signs with good azimuthal coverage using a grid search of all possible orientations of the two nodal planes and finally inspecting the first ten top-score solutions that best separate dilatational from compressional quadrants. The input data were taken from national, international or station bulletins, except for the March 4, 1977 main event whose solution was not re-determined and corresponds to shock E_1 from Räkers and Müller (1982).

Results

Intermediate-depth earthquakes

After searching the stress model space in two steps, we found the best-fitting model presented in Fig. 3, with relative values of principal stresses $\sigma_1 = -0.67\ \sigma_3$ and $\sigma_2 = -$

Table 1. Intermediate-depth earthquakes used in this study. γ is the smallest misfit angle for the two nodal planes, and φ_s and δ are their strike and dip angles, respectively

No.	Date	Origin time	Lat.N (°)	Lon.E (°)	h (km)	M	Nodal planes					Source[a]	No. of P sings	Score (%)
							φ_s (°)	δ (°)	φ_s (°)	δ (°)	$\|\gamma\|$ (°)			
1	340329	20:06	45.8	26.5	90	6.2	200	66	317	45	4	RO'80	33	97
2	400624	09:17	45.9	26.6	115	5.5	220	58	32	32	1	RO'80	27	100
3	401022	06:37	45.8	26.4	122	6.5	223	61	49	30	3	RO'80	57	97
4	401110	01:39	45.8	26.7	133	7.4	224	62	73	31	8	RO'80	58	93
5	450907	15:48	45.9	26.5	75	6.5	224	60	39	30	0	RO'80	30	93
6	451209	06:08	45.7	26.8	80	6.0	134	63	359	36	24	RO'80	24	96
7	480529	04:48	45.8	26.5	140	5.7	196	48	25	42	1	RO'80	33	91
8	550501	21:22	45.5	26.3	135	5.4	103	51	347	61	22	RO'80	28	86
9	600126	20:27	45.8	26.8	140	5.0	155	32	332	58	2	RO'80	53	83
10	601013	02:21	45.7	26.4	160	5.5	163	40	343	50	5	RO'80	47	89
11	630114	18:33	45.7	26.6	133	5.4	146	36	326	54	2	RO'80	54	80
12	650110	02:52	45.8	26.6	120	5.4	348	50	156	41	9	RO'80	54	83
13	661015	06:59	45.6	26.4	140	5.1	134	84	286	7	3	RO'80	39	80
14	730820	15:18	45.7	26.5	73	5.5	262	23	27	80	11	RO'80	49	82
15	731023	10:50	45.7	26.5	170	5.1	117	56	331	39	5	RO'80	34	82
16	740717	05:09	45.8	26.5	145	5.4	216	26	82	72	21	RO'80	55	84
17	761001	17:50	45.7	26.5	146	5.5	169	43	333	48	2	RO'80	85	85
18	770304	19:21	45.8	26.8	93	5.0	275	78	78	12	8	RO'80	61	87
19	770304	19:26	45.8	26.8	93	7.2	238	76	8	21	10	RM'82	78	99
20	781002	20:28	45.7	26.7	140	5.3	131	34	316	56	5	RO'80	108	85
21	790531	07:28	45.6	26.4	120	5.4	233	80	124	27	5	RO'80	89	83
22	790911	15:36	45.6	26.5	158	5.4	210	13	12	77	2	RO'80	100	87
23	810718	00:03	45.7	26.4	146	5.3	184	46	92	88	15	RCO'81	106	78
24	820516	04:03	45.4	26.4	201	4.0	206	81	298	75	15	RO'82	20	82
25	830125	07:34	45.7	26.7	156	5.3	84	50	323	58	18	This paper	72	86
26	850801	14:35	45.8	26.5	107	5.3	200	76	298	61	0	OA'85	86	86
27	860830	21:28	45.5	26.5	134	6.8	235	65	73	24	5	RO'87	232	87

[a] *RO'80* Radu and Oncescu (1980); *RM'82* Räkers and Müller (1982); *RCO'81* Radu et al. (1981); *RO'82* Radu and Oncescu (1982); *OA'85* Oncescu and Apolozan (1985); *RO'87* Radu and Oncescu (1987)

Table 2. Crustal earthquakes used in this study. γ is the smallest misfit angle for the two nodal planes, and φ_s and δ are their strike and dip angles, respectively

| No.	Date	Origin time	Lat.N (°)	Lon.E (°)	h (km)	M	Nodal planes					Source[a]	No. of P signs	Score (%)
							φ_s (°)	δ (°)	φ_s (°)	δ (°)	$\|\gamma\|$ (°)			
1	590531	12:15	45.7	27.2	35	5.2	40	17	149	84	24	RO'80	41	88
2	600104	12:21	44.6	27.0	41	5.4	138	40	271	60	18	RO'80	35	74
3	690418	20:38	45.3	25.1	10	5.2	137	83	231	60	14	RO'80	38	79
4	750208	08:21	45.1	26.0	23	4.7	144	74	48	70	12	RO'80	20	80
5	750307	04:13	45.9	26.6	21	5.1	237	83	143	60	3	RO'80	39	77
6	770305	00:00	45.3	27.1	10	4.3	106	86	13	53	2	RO'80	20	88
7	800911	23:24	45.4	28.2	15	4.7	282	89	12	90	8	RO'80	45	76
8	801208	19:51	44.4	27.2	15	4.0	331	89	240	45	1	RCO'81	23	96
9	811113	09:07	45.2	29.0	10	5.2	314	57	171	39	4	RCO'81	81	73
10	830221	18:03	45.3	27.1	19	4.5	234	63	18	32	2	OA'84	20	95
11	860427	00:04	45.5	27.1	26	5.0	226	44	30	47	2	OT'87	95	90
12	860427	00:47	45.5	27.1	19	3.0	294	62	159	37	10	OT'87	15	93

[a] *RO'80* Radu and Oncescu (1980); *RCO'81* Radu et al. (1981); *OA'84* Oncescu and Apolozan (1984); *OT'87* Oncescu and Trifu (1987a)

0.33 σ_3 ($\sigma_2 = 0.5\,\sigma_1$). This model has an average misfit (absolute value of rotation angle about any axis) of 7.7° with a 95% confidence limit of 11.6°. If the three events that do not fit the model (with misfits greater than 20° and marked with a rectangle in Fig. 1) are removed, the average misfit is reduced to 5.3°. Of the other 24 events, 5 have misfits between 10° and 20° and the remaining 19 fit the stress model within a few degrees. Errors of only several degrees are less than the uncertainty of the focal mechanism determinations, which in this case are estimated to be of the order of 10°.

Crustal events

Again, after searching the stress model space in two steps, we found the best-fitting model presented in Fig. 4, with
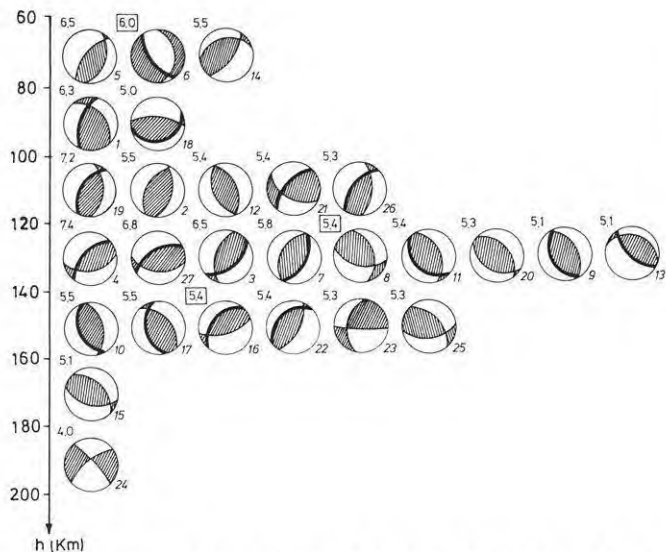
Fig. 1. Stereographic projections of the lower hemisphere of fault-plane solutions for 27 intermediate-depth earthquakes. Magnitudes are indicated near each solution, as well as the corresponding sequene numbers from Table 1. Within each depth interval the earthquakes are ordered with decreasing magnitude; the *first column* may be regarded as a variation of maximum magnitude with depth. *Thick curves* denote identified fault planes (see text)
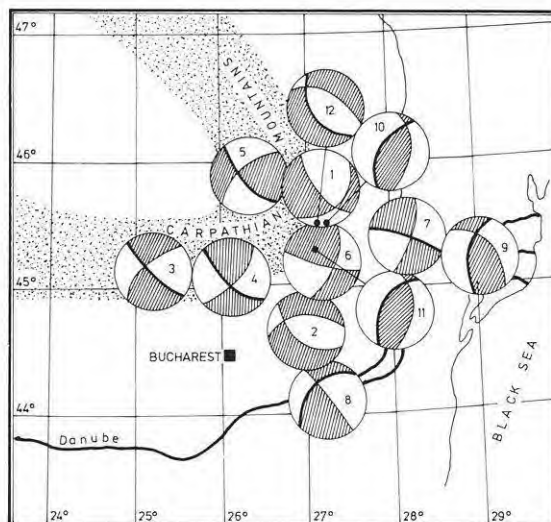
Fig. 2. Stereographic projections of the lower hemisphere of fault-plane solutions for 12 crustal earthquakes. The projections are centred on the epicentres, except where otherwise indicated. *Thick curves* denote identified fault planes (see text). *Numbers* correspond to those from Table 2
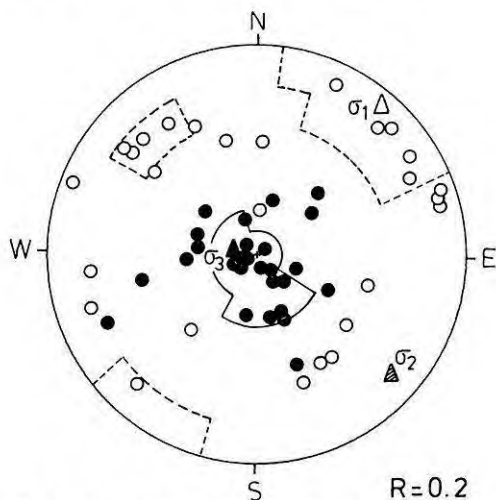
Fig. 3. Principal stress axes (*triangles*), individual P axes (*open circles*) and T axes (*full circles*) for Vrancea intermediate-depth region. Stereographic projections of the lower hemisphere are used. *Contours* indicate 95% confidence regions for σ_1 (*dotted line*) and σ_3 (*solid line*) axes
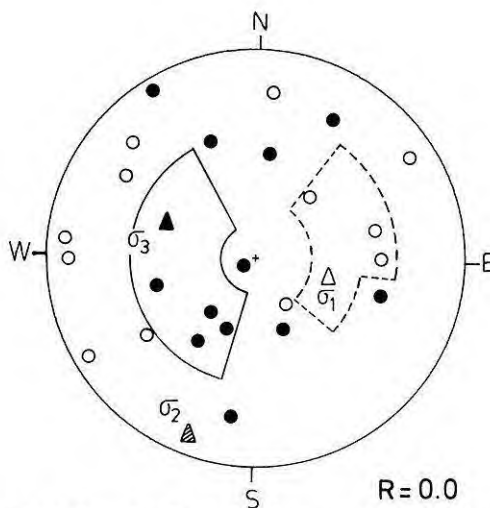
Fig. 4. Same as Fig. 3, but for crustal earthquakes

relative values of principal stresses $\sigma_1 = \sigma_2 = -0.5\,\sigma_3$. This model has an average misfit of 8.4° with a 95% confidence limit of 17.9°. One event has a misfit greater than 20°; if this one is removed, the average misfit is reduced to 6.3°. Of the remaining *11* events, three have misfits between 10° and 20°. The uncertainty of focal mechanism determinations for these crustal events is estimated to be about 15°–20°, so that the fit seems reasonably good.

Discussion

On the basis of this analysis we arrive at the following interpretation concerning the intermediate-depth seismic re-gion. (1) the minimum compression axis (σ_3) acts vertically, as was observed by all previous investigators. (2) The maximum compression axis (σ_1) acts in a NE–SW direction, the direction of the paleo-subduction in Eastern Carpathians, as was pointed out by Bleahu et al. (1973) from volcanological data and by Oncescu et al. (1984) from seismological data. (3) The intermediate stress axis (σ_2) has also a negative sign and acts in a SE–NW direction, the direction of P axes of all strong and most moderate earthquakes; it follows that there are pre-existing planes of weakness on which at least strong and moderate events occur, as suggested by Constantinescu and Enescu (1984). On the other hand, small events with the same orientation of the principal strain axes tend to have high values of fracture energy per unit area of the fault (Oncescu, 1986), a feature generally associated with fresh fracture of rocks. The pattern is not very far from a bi-axial state of stress, as was

first observed by Oncescu and Trifu (1987b) from a statistical analysis of principal strain axes of 120 small earthquakes. A cause of compression along the σ_2 axis (SE–NW) could be the advancement of the Black Sea or Moesian platelet. (4) There is no strong requirement that the stresses are heterogeneous; the few events that do not fit the model are of moderate magnitudes and scattered in space. Following Gephart (1985), we tried to discriminate between the two nodal planes exploiting the fact that the null (B) axes from focal mechanisms are generally not parallel to the σ_2 axis. The choice was made only when the differences in misfits were greater than 10°. For two events, the identified fault planes are coincident with those independently determined by Müller et al. (1978) for the March 4, 1977 M7.2 earthquake and by Trifu and Oncescu (1987) for the August 30, 1986 M6.8 earthquake. These two cases give significance to the other fault-plane identifications, so that one can conclude that (5) when the nodal planes strike NE–SW the rupture plane is that one dipping toward NW, and when the nodal planes strike NW–SE the rupture planes plane is that one dipping toward SW (with two exceptions, the M6.5 and M5.8 events between 120 and 140 km depth).

As to the crustal earthquakes, we obtained that: (1) the most vertical prinicpal stress is the maximum compression (σ_1) axis. (2) The intermediate stress axis (σ_2) equals the σ_1 axis in magnitude (a pure bi-axial stress state), so that their orientation is difficult to determine. Moreover, it is in this situation that the greatest diversity in nodal plane orientations is observed (Harmsen and Rogers, 1986), a feature that can be noticed from Fig. 2. (3) The stress tensor within the crust appears to be quite homogeneous. (4) The clear difference between the stress tensor within the crust and the stress tensor in the intermediate-depth region supports the hypothesis of the existence of a gravitationally sinking slab now decoupled from the crust. Again, following Gephart (1985) and observing that B axes from focal mechanisms are generally not coplanar with the equal principal stress axes, we tried to identify the rupture plane in cases where the differences in misfits were greater than 10°. In all five cases where the fault plane was known independently (although not introduced specifically in the stress inversion), the agreement was perfect.

In conclusion, although this method does not take into consideration stress magnitudes, many interesting new results were obtained (and old results confirmed or proved) about the stress tensor in Vrancea region, which on the basis of P, B, T axes alone could not be inferred, at least not so elegantly and straightforwardly.

References

Bleahu, M.D., Boccaletti, M., Manetti, P., Peltz, S.: Neogene Carpathian Arc: a continental arc displaying the features of an 'Island Arc'. J. Geophys. Res. 78, 5025–5032, 1973

Constantinescu, L., Enescu, D.: A tentative approach to possibly explaining the occurrence of the Vrancea earthquakes. Rev. Roum. Géol. Géophys. Géogr. Géophys. 28, 19–32, 1984

Gephart, J.W.: Principal stress directions and the ambiguity in fault plane identification from focal mechanisms. Bull. Seismol. Soc. Am. 75, 621–625, 1985

Gephart, J.W., Forsyth, D.W.: An improved method for determining the regional stress tensor using earthquake focal mechanism data: application to the San Fernando earthquake sequence. J. Geophys. Res. 89, 9305–9320, 1984

Harmsen, S.C., Rogers, A.M.: Inferences about the local stress field from focal mechanisms: application to earthquakes in the Southern Great Basin of Nevada. Bull. Seismol. Soc. Am. 76, 1560–1572, 1986

McKenzie, D.P.: The relation between fault plane solutions for earthquakes and the directions of principal stresses. Bull. Seismol. Soc. Am. 59, 591–601, 1969

Müller, G., Bonjer, K.P., Stöckl, H., Enescu, D.: The Romanian earthquake of March 4, 1977. I Rupture process inferred from fault plane solution and multiple-event analysis. J. Geophys. 44, 203–218, 1978

Oncescu, M.C.: Relative seismic moment tensor determination for Vrancea intermediate depth earthquakes. Pure Appl. Geophys. 124, 931–940, 1986

Oncescu, M.C., Apolozan, L.: The earthquake sequence of Rîmnicu Sărat, Romania, of 21–22 February 1983. Acta Geophys Pol 32, 231–238, 1984

Oncescu, M.C., Apolozan, L.: The seismic doublet from Vrancea region of August 1, 1985 (in Romanian). Stud. Cerc. Geol. Geofiz. Geogr. Geofiz. 24, 12–16, 1985

Oncescu, M.C., Trifu, C.I.: A large seismic sequence on April 27–29, 1986 in Vrancea foredeep. Rev. Roum. Géol. Géophys. Géogr. Géophys. 31, 1987a (in press)

Oncescu, M.C., Trifu, C.I.: Depth variation of moment tensor principal axes in Vrancea (Romania) seismic region. Ann. Géophys. 5B, 149–154, 1987b

Oncescu, M.C., Burlacu, V., Anghel, M., Smalberger, V.: Three-dimensional P-wave velocity image under the Carpathian Arc. Tectonophysics 106, 305–319, 1984

Radu, C., Oncescu, M.C.: Focal mechanism of Romanian earthquakes and their correlation with tectonics. I. Catalogue of fault plane solutions (in Romanian). Report CFPS/CSEN 30.78.1, 1980

Radu, C., Oncescu, M.C.: A note on the deep Vrancea earthquake of May 16, 1982 (in Romanian). Report CFPS/CSEN 30.81.8, 1982

Radu, C., Oncescu, M.C.: Focal process of August 30, 1986 Vrancea earthquake (in Romanian). Report CFPS/CSEN 30.86.3, 1987

Radu, C., Crişan, E., Oncescu, M.C.: Fault plane solutions of Romanian earthquakes occurred in 1981 (in Romanian). Report CFPS/CSEN 30.81.8, 1981

Räkers, E., Müller, G.: The Romanian earthquake of March 4, 1977. III. Improved focal model and moment determination. J. Geophys. 50, 143–150, 1982

Ritsema, A.R.: The earthquake mechanisms of the Balkan region. UNDP Project REM/70/172, UNESCO, 1974

Roman, C.: Seismicity in Romania – evidence for the sinking lithosphere. Nature 228, 1176–1178, 1970

Trifu, C.I., Oncescu, M.C.: Fault geometry of August 30, 1986 Vrancea earthquake. Ann. Géophys. 6B, 1987 (in press)